Numerical Methods in Civil Engineering, 6-3 (2022) 92-102

Numerical Methods in Civil Engineering

Journal Homepage: https://nmce.kntu.ac.ir/

A Numerical Laboratory for Simulation of Flanged Reinforced Concrete Shear Walls

Alireza Khaloo[*], Mohammad Tabiee[**], Hatef Abdoos[***]

ARTICLE INFO

RESEARCH PAPER

Article history:
Received:
September 2021.
Revised:
November 2021.
Accepted:
December 2021.

Keywords:
Flanged RC shear wall
Numerical simulation
Finite Element Method
Shell element
Shear-lag effect

Abstract:

The present paper establishes the Flanged reinforced concrete (RC) Shear Wall Laboratory (FlashLab) Software Program. Despite their extensive applications in recent years, flanged RC shear walls have rarely been experimentally and numerically studied, mainly due to the difficult and time-consuming fabrication of experimental samples, numerical models, and also their analysis. FlashLab is a finite element method (FEM)-based simulator of flanged RC shear walls. Drawing on ABAQUS, FlashLab employs shell elements with longitudinal and transverse reinforcements to accurately and rapidly model the cyclic behavior of flanged RC shear walls. The FlashLab algorithms are on the basis of the Python programming language and can examine flanged RC shear walls, with a general cross-section, which make it possible to parametrically investigate various variables. In order to validate FlashLab, this paper numerically simulates T-, H-, and L-shaped RC shear walls and compares the results to the experimental data, indicating good agreement between the numerical and experimental results to an extent that the proposed numerical laboratory is capable of predicting the backbone curve with an accuracy more than 90 percent. Moreover, to verify the simulation performance of FlashLab, the shear-lag effect was parametrically studied as a unique phenomenon in flanged RC shear walls. The findings of the current study clearly demonstrates the robustness and efficiency of FlashLab in the behaviour simulation of flanged RC shear walls.

Nomenclature

ε_{50c}	Strain corresponding to the stress of $0.50f_c'$ after attaining the maximum compressive strength of concrete
ε_{20c}	Strain corresponding to the stress of $0.20\,f_c'$ after attaining the maximum compressive strength of concrete
ε_{sh}	Strain at the onset of hardening stage
ε_{su}	Strain corresponding to the ultimate strength of steel reinforcement
ε_{sy}	Strain corresponding to the yield stress of steel reinforcement
ε_t	Strain corresponding to the ultimate tensile strength of concrete
ε_{tu}	Ultimate tensile strain of concrete
η	Viscosity parameter
θ_u	The ratio of the axial displacement to the maximum axial deformation
σ_c	Compression stress in concrete element
ψ	Dilation angle
A_g	Cross-sectional area of the wall
b_{CL}, b_{CV}	Longitudinal and transverse bars diameter in the confined area
$b_{fbL}, b_{fbR}, b_{ftL}, b_{ftR}$	Widths of the left-side bottom flange, right-side bottom flange, left-side top flange, and right-side top flange
b_L, b_V	Longitudinal and transverse bars diameter
C	Shear center of the wall section
d_b	Bar diameter
d_c	Confined length of the section
d_{cv}	Spacing of the transverse bars in the confined area
d_L, d_V	Spacing of the longitudinal and transverse bars
E_c	Elasticity modulus of concrete

E_s	Elasticity modulus of steel reinforcements
e_c	Clear cover
e_x, e_y	Eccentricity of the lateral loads in *y*- and *x*-directions from the shear center
f_u	Ultimate stress of steel reinforcement
f_y	Yield stress of steel reinforcement
f_c'	Compressive strength of concrete
f_t'	Tensile strength of concrete
G	Centroid of the wall section
H	Height of the wall
h	Shear wall section height
N	Applied axial loading
m	Eccentricity
t_{fb}, t_{ft}, t_w	Thickness of the bottom flange, top flange, and web
V_x, V_y	Lateral loads in *x*- and *y*-directions
(x_c, y_c)	Shear center coordinate
(x_G, y_G)	Centroid coordinate of the section

1. Introduction

Reinforced concrete (RC) shear walls have increasingly been employed in the construction industry, since it is important to improve the lateral load resistance of structures and restrict their lateral deformation, particularly in high-rise structures. Although a majority of RC shear walls have rectangular sections, flanged RC shear walls are sometimes used due to the distinct architecture of the building or to enhance stiffness in specific structures. Such walls are constructed by connecting several walls of rectangular sections which demonstrate distinct structural performance in comparison with conventional rectangular RC shear walls, such as the well-known shear-lag phenomenon. In fact, once a flanged section is subjected to lateral loads, the shear flow increases the axial strain and stress in the web-flange conjunction. This phenomenon is known as shear-lag. As a result, the Bernoulli-Euler assumption does not hold for flanged shear walls, and in turn, the flexural stiffness and capacity of the section will be reduced [1].

* *Corresponding Author: Distinguished Professor, Department of Civil Engineering, Sharif University of Technology, Tehran, Iran, Email: Khaloo@sharif.edu*
** *M.Sc. student, Department of Civil Engineering, Sharif University of Technology, Tehran, Iran.*
*** *Ph.D. student, Department of Civil Engineering, Sharif University of Technology, Tehran, Iran.*

Due to such unique behavior of flanged shear walls, extensive experimental as well as numerical studies have been conducted to provide better understanding of the performance of non-rectangular RC shear walls. Moreover, due to the complications that exist in the fabrication and testing of experimental samples [2], more contribution towards the study of flanged RC shear walls is devoted to numerical studies. In what follows, the numerical methods used to study RC shear walls are reviewed.

Numerical models employed in the simulation of RC shear walls can be classified into the micro- and macro-models. Galal and El-Sokkary (2008) reviewed micro-models of RC shear walls (e.g., finite element method (FEM) and fiber models), and macro-models (e.g., lumped plasticity models, multi-axial spring models and combined models). They evaluated these methods in terms of performance and explored the main factors which affect the accuracy of these methods. It was concluded that the FEM simulation of shear walls seems to be more popular among researchers and can also contribute to higher performance and accuracy [3].

Apart from the conventional models in the simulation of RC shear walls, a number of researchers developed new, innovative numerical techniques in order to achieve more simple models with lower computational efforts. To simulate RC shear walls, Chen and Kabeyasawa (2000) employed two linear boundary elements (i.e., two axial springs) and a plane-stress panel. They compared the results to the experimental data of a T-shaped shear wall. It was observed that the proposed method not only reduced the computational effort and costs, but could also offer good agreement with the experimental data [4] (Fig. 1).

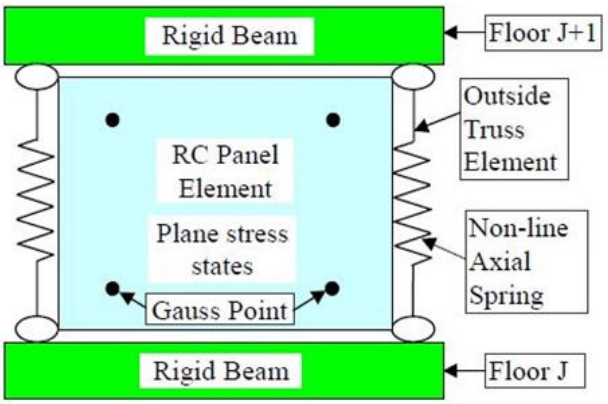

Fig. 1: Macro-element model for RC wall member [4]

Brueggen and French (2010) proposed a new, simple F-S-SP integration model for the simulation of non-rectangular structural walls. The F-S-SP model could present the load-displacement curve of a non-rectangular RC wall and also detect the damage degrees. The results were compared to the experimental data of eight specimens which demonstrate acceptable performance of the proposed model [5].

As mentioned, various numerical methods have been proposed for the analysis of RC shear walls. However, most of the numerical studies on non-rectangular RC shear walls were conducted using FEM, and therefore, FEM-based numerical investigations on non-rectangular RC shear walls are the center of attention, which will be reviewed in the following sections.

Kwan (1996) studied the effects of the shear-lag on box-shaped walls adopting FEM to accurately estimate the stress and strain distributions of the section using relatively fine mesh and a parametric study [6].

Arnott (2005) analyzed rectangular and non-rectangular RC shear walls in high- and mid-rise structures employing FEM based on the shell and beam elements. In this investigation, the computational effort and performance of the shell and beam elements were compared, and it was found that the modeling of shear walls using shell elements can offer low computational effort and acceptable performance [7].

Palermo et al. (2007) reported numerical analysis results of L-, T-, H-, and U-shaped RC shear walls. They demonstrated the satisfactory performance of FEM in the simulation process of non-rectangular shear walls. It was also revealed that the codes were not efficient enough in estimating the effective flange width of the shear wall. Furthermore, a significant effective flange width difference was observed between the wall flanges under tensile and compressive loads. It should be noted that the numerical results were in good agreement with the experimental data in this investigation [8].

Kheyroddin and Mortezaei (2007) numerically investigated the parameters influencing the effective flange width of a shear wall employing the NONLACS2, nonlinear finite element program. They found that width and height of the wall, axial load, and inter-story drift are the key parameters affecting the effective width of the wall [9].

Hoult (2019) studied the effects of the shear-lag phenomenon on the axial stress and strain distributions of C-shaped (U-shaped) RC shear walls through the nonlinear modeling of 54 samples adopting FEM in the Vector3. Then, the numerical results were compared with the experimental data and good agreement was achieved. In addition, on account of the results, an equation was proposed to estimate the effective flange width of C-shaped RC shear walls with satisfactory accuracy [10] (Fig. 2).

Lu and Li (2020) parametrically examined T-shaped shear walls and proposed equations to estimate the axial stress distribution and effective flange width. The comparison of the results with the nonlinear FEM modeling indicates good agreement [11].

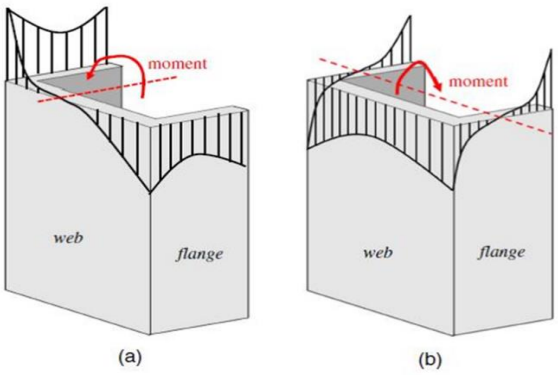

Fig. 2: Expected strain distributions for bending in a C-shaped shear wall [10]

Most FEM-based numerical studies on non-rectangular RC shear walls simulated the wall in detail. Although this scheme can improve accuracy of the modeling, such approaches significantly increase the computational time and effort. However, to identify the unique characteristics of non-rectangular RC shear walls and develop accurate equations, it is required to examine a large number of samples. Moreover, most studies on flanged shear walls mainly focused on T-, U-, and L-shaped sections, while there are more cross-section shapes of flanged shear walls.

This paper introduces the Flanged Shear Wall Laboratory (FlashLab) and describes its algorithms and features. The performance of FlashLab is then validated comparing the numerical simulation results of T-, H-, and L-shaped shear walls to the experimental data, evaluating its accuracy in the performance estimation of the wall.

As previously mentioned, many experimental studies were conducted on non-rectangular RC shear walls. However, a number of researchers adopted improper techniques; therefore, their results would not be a reliable reference to validate a model [10].

Ma (2016) experimentally subjected 12 RC shear walls of L-, H-, and T-shaped sections to axial and cyclic lateral loads. He studied the seismic performance of the walls in terms of cracking patterns, failure mechanisms, hysteresis responses, deformation components, and strain profiles. Thereafter, three-dimensional shear wall models were simulated using FEM, and then, the results were validated through comparison with the experimental data [12]. It should be noted that the present paper utilizes the experimental data of Ma (2016) to validate FlashLab in the simulation process of non-rectangular RC shear walls.

FlashLab has been developed based on the Python programming language and with the aid of shell elements in ABAQUS software. It simulates flanged RC shear walls with an arbitrary cross-section. FlashLab can also perform parametric studies analyzing significant number of numerical samples. In order to demonstrate the performance of FlashLab, this paper parametrically examines the shear-

lag phenomenon in flanged RC shear wall using FlashLab to discuss the results and conclude the work.

2. Introduction of FlashLab program

2.1 The general execution procedure of the program

FlashLab is a numerical modeling program capable of simulating flanged RC shear walls with general geometry, boundary conditions, and loading shown in Fig. 3, implementing the finite element method and shell elements.

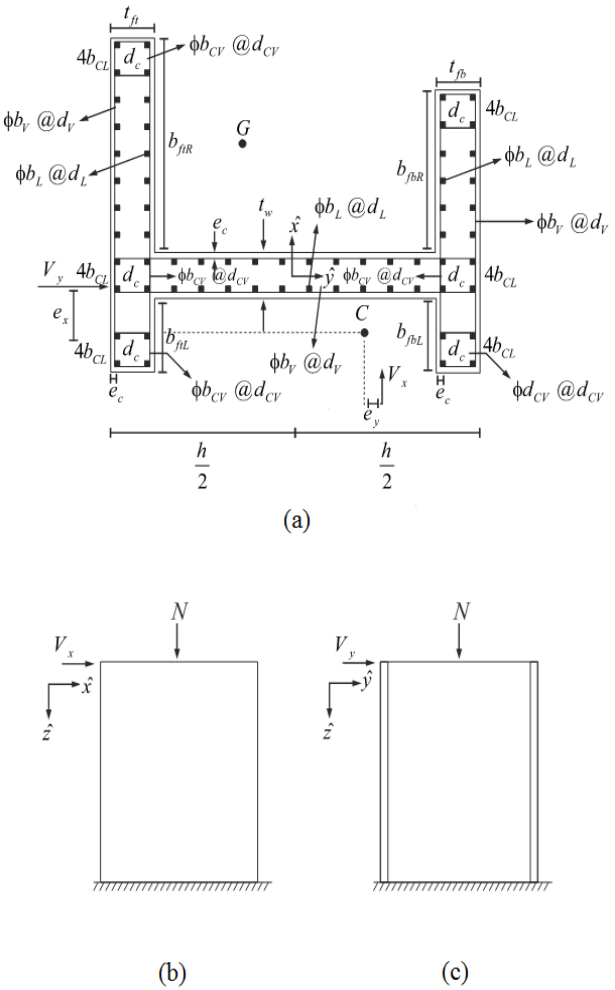

Fig. 3: The loading condition and general geometry of flanged sections in FlashLab

Utilizing a simple structure, this program allows producing and analyzing numerical samples in large quantities to perform comprehensive parametric studies on the input variables with favorable accuracy within a short duration. Using Python programming, the program at first receives the required user input data, including geometrical characteristics and material properties. Thereafter, the variable subjected to the parametric study is introduced along with its range and number of samples. In the next step, given the inputs received from the user, each of the modules of Part, Property, Assembly, Step, Load, Mesh and Job in the ABAQUS software are automatically set as demonstrated in the flowchart (see Fig. 4). The samples are simulated accordingly. After termination of each modeling, its results are obtained and depending on the required parameters introduced by the user, the outputs are extracted from the results and saved.

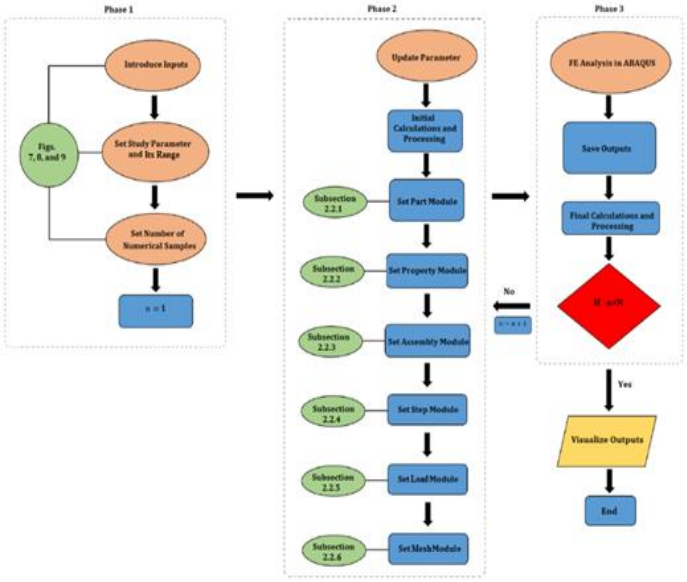

Fig. 4: The flowchart of the execution procedure of the FlashLab program

The following sub-sections briefly describe the settings implemented in each module of ABAQUS software through the FlashLab program.

2.2 Settings of the ABAQUS modules

2.2.1 *Part module*

Given the inputs corresponding with the geometrical characteristics of the wall in the first phase of the FlashLab, this program defines the geometry of the structure as shown in Fig. 5, employing the 3D shell elements in the Part module.

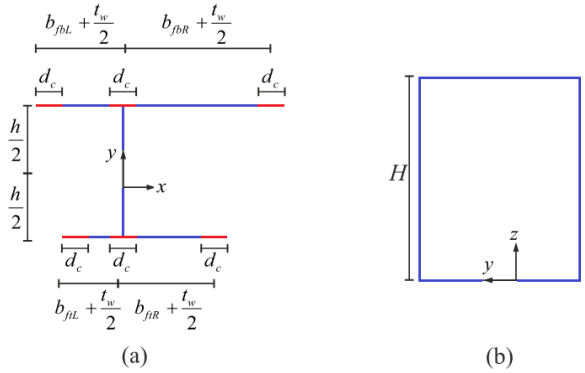

Fig. 5: The geometry of the flanged shear wall simulated in ABAQUS software

It is worth noting that, if any of the parameters b_{ftL} , b_{ftR} , b_{fbL} , and b_{fbR} are lower than d_c , the confined area does not form in the corresponding part of the wall flange. Accordingly, using the FlashLab program, different types of flanged shear walls can readily be created and examined (Fig. 6).

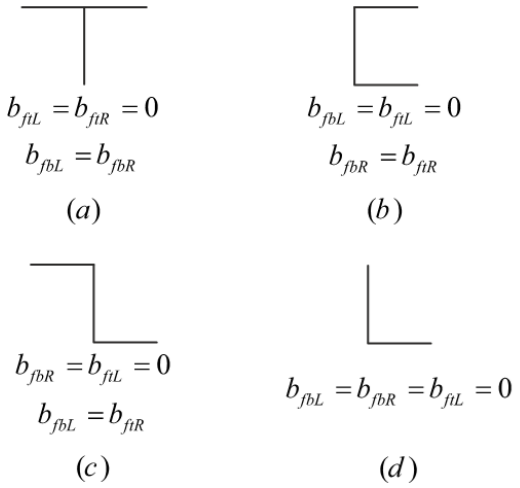

Fig. 6: The flanged RC shear walls with conventional sections: (a) T-shaped section, (b) U-shaped section, (c) Z-shaped section, and (d) L-shaped section

2.2.2 *Property module*

The behavior of the materials, including concrete and steel reinforcements under tension and compression and their damage properties are determined based on the property inputs. Moreover, the thicknesses of the shell elements and reinforcement bars configuration in the walls are also determined.

To model the nonlinear behavior of reinforcement bars under tension and compression, the trilinear model of the steel stress-strain curve is employed (Fig 7). It is worth bearing in mind, that all the parameters of the stress-strain curve are input at the beginning of the process. It should also be noted that the curve plotted in Fig. 7 is symmetric with respect to the origin of the coordinate system.

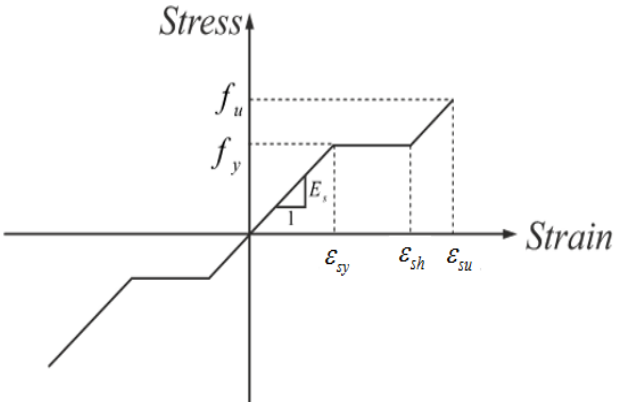

Fig. 7: The stress-strain curve of steel reinforcements in FlashLab

Additionally, the simulation of concrete materials requires two distinct properties in both the tensile as well as the compressive regions of the stress-strain curve. Hence, this study adopted the compressive concrete stress-strain curve proposed by Kent and Park for the confined concrete elements with rectangular hoops [12, 14]. In addition, as shown in Fig. 8, the bilinear model is employed to simulate the tensile behavior of concrete materials [13].

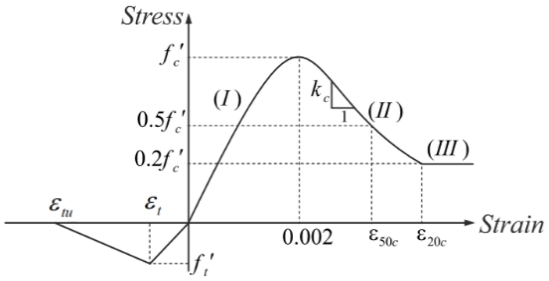

Fig. 8: Stress-strain curve of concrete in FlashLab

The equations corresponding to zones I, II, and III in the stress-strain curve of Fig. 8 are formulated as follows [12-14]:

Zone I:

$$\sigma_c = f_c'[\frac{2\varepsilon_c}{0.002} - (\frac{\varepsilon_c}{0.002})^2] \quad (1)$$

Zone II:

$$\sigma_c = f_c'[1 - \frac{k_c}{f_c'}(\varepsilon_c - 0.002)] \quad (2)$$

where

$$k_c = \frac{0.5f_c'}{\varepsilon_{50c} - 0.002} \quad (3)$$

$$\varepsilon_{50c} = \frac{20670 + 0.002f_c'}{f_c' - 6890000} + \frac{3}{4}\rho_s\sqrt{\frac{b''}{s_h}} \quad (4)$$

In which f_c' (in Pa) represents the characteristic concrete strength.

In order to simulate the nonlinear characteristics of concrete materials and also determine the damage of concrete materials in process of numerical analyses, various models have been proposed. The concrete smeared crashing (CSC) and concrete damage plasticity (CDP) models possess high efficiency and can be applied in the simulation of concrete elements in ABAQUS [15, 16].

It should be noted that the CDP model essentially assumes tensile cracks and compressive crashing to be the two main aspects of the concrete fracture mechanism. Therefore, to simulate the fracture of concrete materials under cyclic tensile-compressive loading, the CDP model is used. As the CDP model allows recovering stiffness during the loading

cycles [17], CDP is employed in FlashLab to simulate the nonlinear behavior of concrete elements and determine the damage characteristics. The considered concrete damage plasticity parameters in FlashLab is presented in table 1.

Table. 1: CDP parameters

ψ	m	f	k	η
30.5°	0.1	1.16	0.667	0.001

In this module, the thicknesses of shell elements and the configurations of transverse and longitudinal reinforcement bars (Fig. 3) are user input data (Fig. 9).

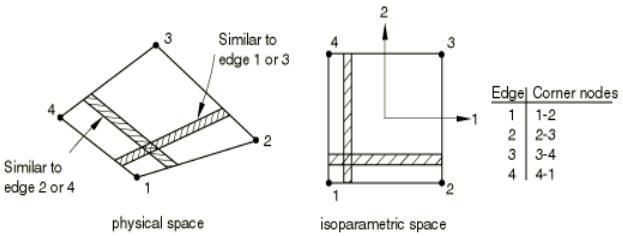

Fig. 9: Rebar layer definition in a three-dimensional shell or membrane [17]

2.2.3 *Assembly module*

FlashLab models the wall as an integrated structure. Hence, it is not required to use settings to assemble components in the Assembly module. This module assumes a dependent instance type. As a result, "mesh on part" condition is considered.

2.2.4 *Step module*

FlashLab employs a dynamic-explicit analysis type, and the period is considered to be the time of the cyclic loading. It should be noted that the nonlinear geometric effects are also deemed in FlashLab. In addition, in this module, the output variables to be calculated and saved in the analysis are determined.

2.2.5 *Load module*

Although the boundary conditions and applied loading of RC shear walls may be diverse in general, the common experimental boundary conditions and loading schemes are considered as default to save time in the simulation process, and in turn, the examination of flanged RC shear walls in FlashLab. A cantilever RC shear wall is subjected to strain-controlled cyclic loading condition in *x*- or *y*-directions (Fig. 10). The displacement of the wall follows a load history diagram which is an input by the user.

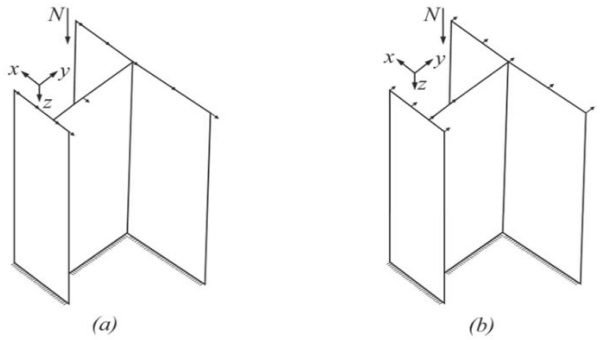

Fig. 10: Boundary conditions of flanged RC shear walls in FlashLab

It is worth noting that, in most simulations, an axial load within the range from $0.05f_c'A_g$ to $0.10f_c'A_g$ was also applied to the centroid of the sections. In FlashLab program, if existing, the axial load is uniformly applied to each edge of the shell element. The value of this uniform loading is obtained from Nt/A_g, in which t is the thickness of the intended shell element and A_g is the cross-sectional area of the wall.

2.2.6 *Mesh module*

The meshing type as well as the number of elements have a significant effect on the FE modeling results [18]. As mentioned in the previous section, the shell elements can offer an accurate estimation of responses under a given loading in the simulation process of RC shear walls. Hence, this study employed four-node general-purpose shell (S4R) elements for the modeling of flanged RC shear walls. The elements were assumed to have an average size of *H*/50 to *H*/10 [19].

It should be noted that the analysis is initiated by saving the user-defined outputs after implementing the settings in ABAQUS. Then, assuming unchanged input parameters, the variable under study is altered, re-performing the simulation. This process is carried out iteratively. The number of iterations is defined by the user at the onset of the process in FlashLab.

3. Validation of FlashLab

To validate FlashLab, the numerical simulation results of T, H-, and L-shaped shear wall models are compared to the experimental data reported by Ma [12]. Figs. 11, 12, and 13 respectively demonstrate the geometries of RC shear walls, configurations of steel reinforcements, and loading history diagrams.

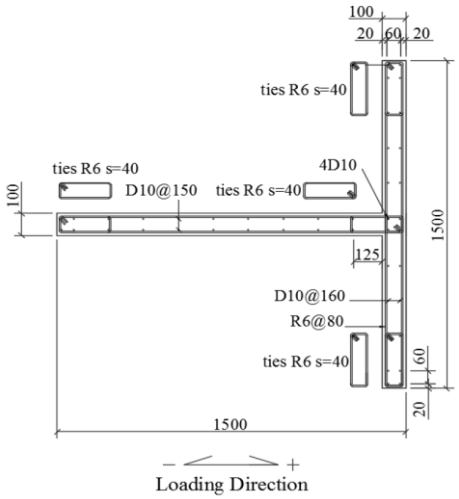

(a)

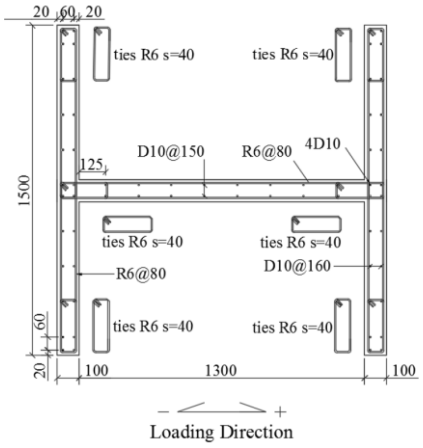

(b)

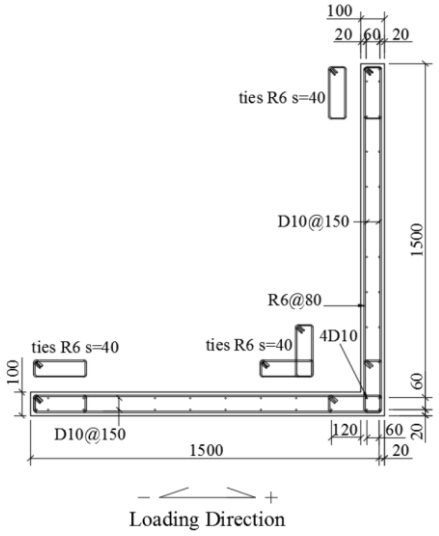

(c)

Fig. 11: Steel reinforcements in: (a) T-shaped, (b) H-shaped, and (c) L-shaped RC shear walls

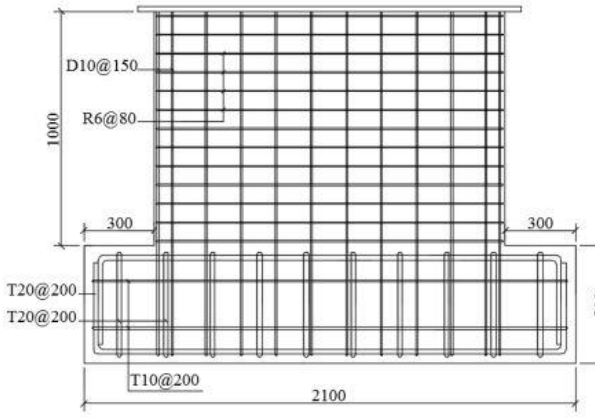

Fig. 12: Vertical view of the shear walls

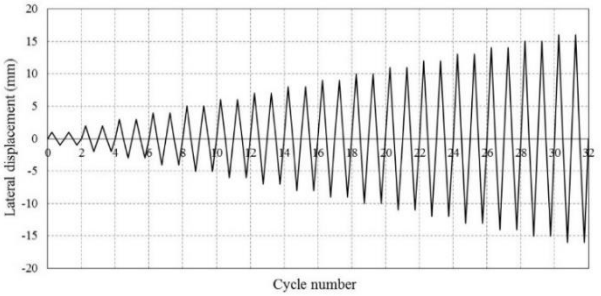

Fig. 13: Loading history

Also, Tables 2 and 3 summarize the properties of concrete materials and reinforcement bars, respectively.

Table. 2: Concrete properties

Sample	f_c'(MPa)	f_t'(MPa)	E_c (GPa)
T-shaped	35.0	3.60	28.2
H-shaped	35.9	3.80	28.6
L-shaped	35.0	3.70	28.3

Table. 3: Reinforcement bar properties

Rebar	d_b (mm)	f_y (MPa)	ε_y	E_s (GPa)	f_u (MPa)
R16	6	335	0.00160	220	507
D10	10	554	0.00252	220	642

The axial loads applied to each of the H-, T-, and L-shaped walls were equal to $7.2f_c'A_g \times 10^{-3}$, $4.8f_c'A_g \times 10^{-3}$, and $7.2f_c'A_g \times 10^{-3}$, respectively. The samples introduced with the mentioned properties were simulated using FlashLab program. Fig. 14 depicts the structure and meshing of the models implemented in the ABAQUS.

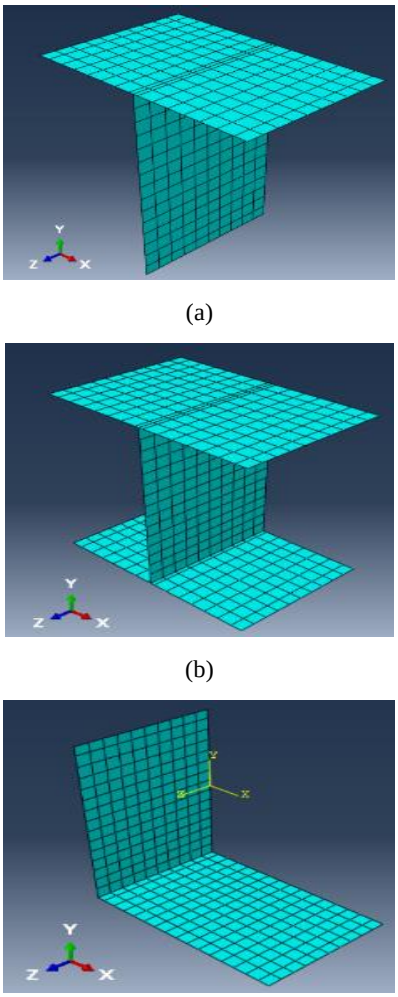

(a)

(b)

(c)

Fig. 14: The modeling of: (a) T-shaped, (b) H-shaped, and (c) L-shaped sample

After the simulation phase terminates, the analysis process initiates. The hysteresis curve of each of the samples under the applied cyclic loading is obtained as an output of the program. On account of the hysteresis curves, the backbone curve is obtained and then simplified bi-linearly for each of the modeled walls. Fig. 15 compares the backbone curves obtained from the numerical simulations using FlashLab program with those attained by the experimental data for each of the H-, T-, and L-shaped walls.

By evaluating Fig. 15, it can be found that the modeling accuracy of the response in the elastic range was very high, and the difference in this range was less than five percent. However, the error in the non-elastic area was less than ten percent on average. Therefore, it can be concluded that FlashLab program offers a satisfactory performance in simulating the behavior of non-rectangular RC shear walls.

In the next section, in order to evaluate the efficiency of the FlashLab program in simulation and parametric study on numerous samples of flanged RC shear walls, the effect of the spacing of longitudinal and transverse bars on the axial deformation induced by the shear-lag is investigated.

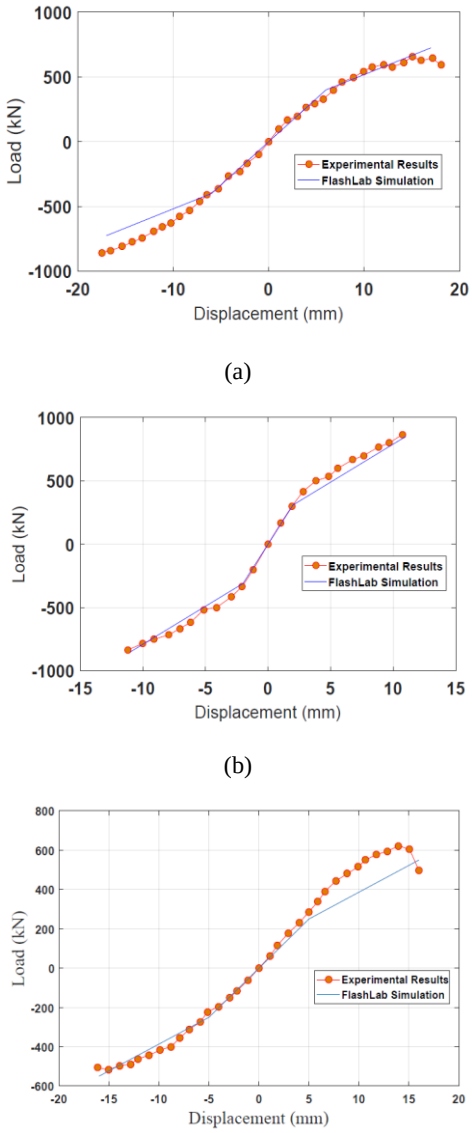

(a)

(b)

(c)

Fig. 15: A comparison between the backbone curves obtained from the experimental results and numerical simulations of a) T-shaped, b) H-shaped, and c) L-shaped walls

4. Parametric studies using FlashLab program

As mentioned earlier, for the parametric study in FlashLab program, all the input variables are deemed to be constant, and only the parameter under examination is altered within the range defined by the user and for the times specified at the first phase of the program. Therefore, in order to investigate the effect of longitudinal and transverse bars on the axial deformation induced by the shear-lag, a flanged RC shear wall with an I-shaped section and asymmetric flanges was considered, as shown in Fig. 16. By changing the spacing of the longitudinal and transverse bars, the variation of the axial deformation in the flanges of the section were assessed.

It is worth noting that while the shear-lag simultaneously affects the axial stress as well as the axial strain of the walls with non-rectangular sections, only the axial displacement was considered in the shear-lag evaluation; since, in the shell elements, the normal stress in the direction perpendicular to the thickness of the plane is ignored.

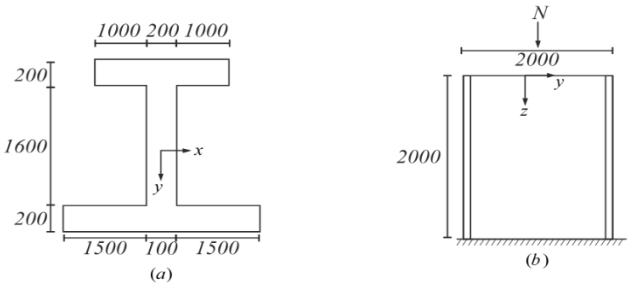

Fig. 16: The geometrical properties of the I-shaped RC shear wall (all dimensions are in mm)

In this section, reinforcement bars of 10 and 12 mm diameter were used as the longitudinal and transverse bars. The dimensions of the confined area as well as the thickness of the concrete cover were $20\,\text{cm}\times 20\,\text{cm}$, and approximately $4\,\text{cm}$, respectively. Tables 4 and 5 summarize the mechanical properties of the materials employed in this sample.

Table. 4: Concrete properties

Sample	f_c'(MPa)	f_t'(MPa)	E_c (GPa)
I-shaped	40	3.9	30.2

Table. 5: Characteristics of reinforcement bars

Rebar	d_b (mm)	f_y (MPa)	ε_y	E_s (GPa)	f_u (MPa)
$\phi 10$	10	300	0.00143	210	450
$\phi 12$	12	400	0.00190	210	600

It should be mentioned that the loading of this sample was also cyclic along *y*-direction, as shown in Fig. 17. Moreover, the spacing of the longitudinal and transverse rebars varied within the ranges of 10-50 cm and 5-25 cm, respectively. A total of 10 samples were considered for the purpose of parametric studies. The output of FlashLab program in these studies was the distribution of the axial deformation at the end of the loading procedure. Therefore, in order to save the time spent on the calculations, the number of applied cycles has been reduced.

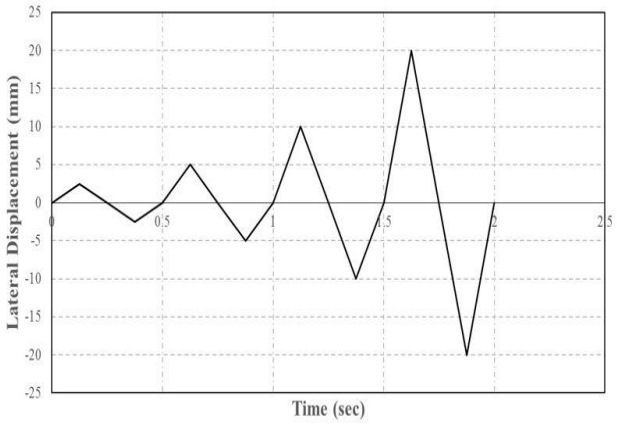

Fig. 17: Loading history

Currently, parametric studies are performed in FlashLab. Fig. 18 indicates the axial displacement contour of the sample. As can be seen, due to shear-lag effect, the highest axial displacement occurred in the web-flange connection at the free end of the wall.

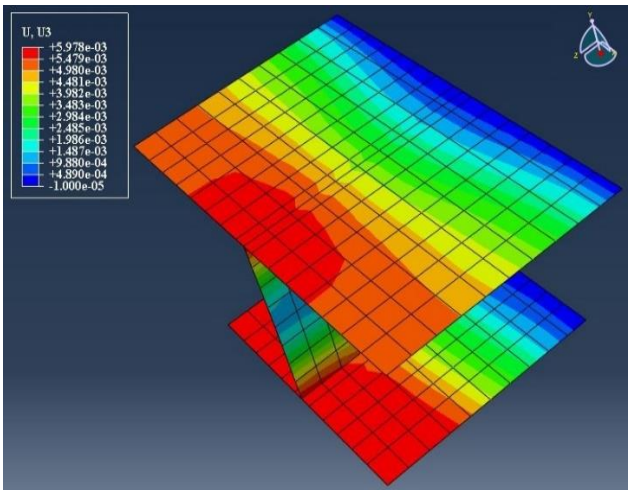

Fig. 18: Axial displacement contour of the I-shaped shear wall with asymmetric flanges

Figs. 19 and 20 plot the maximum axial deformations (MAD) of the section under the applied cyclic loading versus the longitudinal and transverse rebar spacing. Khaloo et al. (2021) analytically studied the effect of shear-lag on an I-shaped concrete shear wall with asymmetric flanges in the elastic region. It is also pointed out that the axial displacement of the section under the shear-lag effect can be a function of the equivalent elasticity modulus of the section [20]. Hence, the maximum axial displacement augments as the spacing of longitudinal and transverse rebar increases (i.e., reduced reinforcement). Thus, the curves plotted in Figs. 19 and 20 were expectedly found to have overall increasing trends.

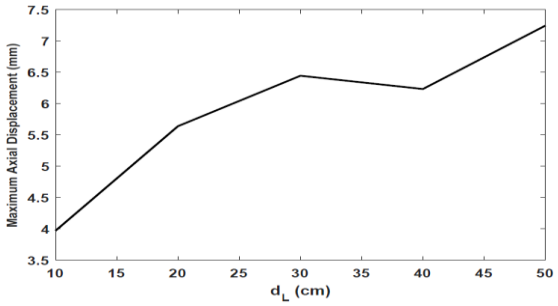

Fig. 19: The maximum axial displacement versus the spacing of the longitudinal bars

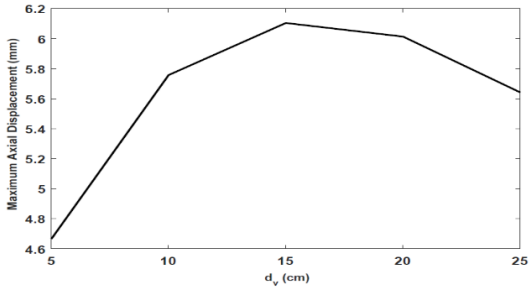

Fig. 20: The maximum axial displacement versus the spacing of the transverse bars

To investigate the distribution of the axial deformation induced in the flanges of the section, function θ_u is defined herein for the bottom flange as the ratio of the axial displacement to the maximum axial deformation. Figs. 21 and 22 plot the distribution of θ_u along the flange versus the longitudinal and transverse rebar spacing.

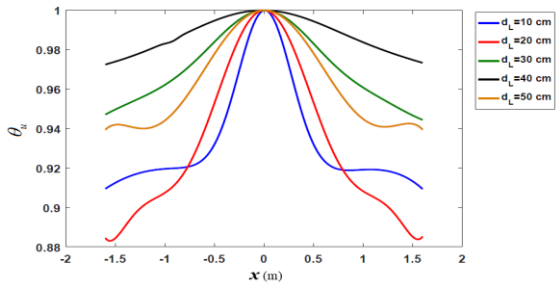

Fig. 21: Axial deformation distribution in the bottom flange versus the spacing of the longitudinal bars

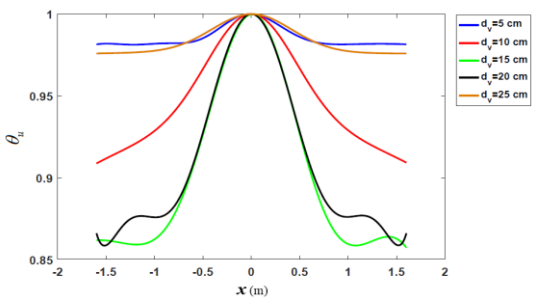

Fig. 22: Axial deformation distribution in the bottom flange versus the spacing of the transverse bars

Based on the results attained by the parametric studies in FlashLab, it can be revealed that both the longitudinal and transverse rebar spacing affect the maximum induced axial displacement and axial displacement distribution in the flange, due to the presence of the shear-lag. According to Figs. 21 and 22, since the maximum difference between the corresponding values of these curves are less than ten percent, and also in practice there is a limited interval for the spacing of the longitudinal and transverse bars; hence, the effect of rebar spacing on the axial displacement is not meaningful for most cases examined in this study.

5. Conclusion

The current study investigated the main structure and performance of a numerical laboratory for the simulation of flanged RC shear walls (FlashLab program). Due to the advancements in the construction technology and ever-increasing use of RC shear walls with non-rectangular sections, many experimental and numerical studies have been performed to identify the behavior of such walls. Numerical studies encounter an essential challenge in constructing detailed models with time-consuming evaluations. To overcome this challenge, FlashLab has been established to analyze flanged RC shear walls.

FlashLab employs the Python programming language to simulate and analyze a variety ranges of flanged RC shear wall models in a short time with the aid of shell elements in ABAQUS software environment. The execution of FlashLab has thoroughly been described, evaluating its accuracy by comparing the results to the experimental data of T-, H-, and L-shaped RC shear walls, and then observing the backbone curve differences below ten percent.

To demonstrate the performance of FlashLab in parametric study, an example was provided to examine the effects of longitudinal and transverse bars spacing on the shear-lag-induced axial deformation. It should be noted that shear lag is unique to flanged RC shear walls, and the effects of rebar configuration on the shear-lag have rarely been evaluated. It was found that an increase in the spacing of longitudinal and transverse bars can significantly affect the maximum induced axial deformations of the section. Furthermore, the relative difference between the minimum and maximum values of MAD when the longitudinal and transverse bar spacing increased, were about 80 and 30 percent, respectively. Despite this significant effect, the longitudinal and transverse bar spacing due to their limited values have negligible effects on the axial deformation distribution along the flanges of the section.

References

[1] Khaloo, A. R., Tabiee, M, Abdoos, H, Shear lag effect on non-rectangular RC shear walls: a review of the literature, 7th

international congress on civil engineering, architecture and urban development, Tehran, Iran.[In Persian]

[2] R. Constantin, K. Beyer, Non-rectangular RC walls: A review of experimental investigations, in: 2nd European Conference on Earthquake Engineering and Seismology, 2014.

[3] Galal, K. and H. El-Sokkary." Advancement in modeling of RC shear walls," in The 14th World Conference on Earthquake Engineering, Beijing, China. 2008.

[4] Chen, S. and T. Kabeyasawa, "Modeling of reinforced concrete shear wall for nonlinear Analysis," 12th WCEE, Auckland, New Zealand, 2000.

[5] Brueggen, B., "Performance of T-shaped reinforced concrete structural walls under multi- directional loading,"Ph.D. thesis, University of Minnesota, 2010.

[6] Kwan, A.K., "Shear lag in shear/core walls," Journal of Structural Engineering, 1996. 122(9): p. 1097-1104.

[7] Arnott, K., "Shear wall analysis- new modelling, same answers," Structural Engineer, 2005. 83(3): p. 20-22.

[8] Palermo, D., A. Abdulridha, and M. Charette, "Flange participation for seismic design of reinforced concrete shear walls," 2007.

[9] Kheyroddin, A. and A. Mortezaei, "Investigation of influential variables in flange effective width of reinforced concrete shear walls,"9th Canadian conference on earthquake engineering, Ottawa, Canada, 2007.

[10] Hoult, R.D., "Shear lag effects in reinforced concrete C-shaped walls," Journal of Structural Engineering, 2019. 145(3): p. 04018270.

[11] Lu, N. and W. Li, "Analytical study on the effective flange width for T-shaped shear Walls," Periodica Polytechnica Civil Engineering, 2020. 64(1): p. 253-264.

[12] Ma, J., "Experimental and analytical investigations on seismic behavior of non- rectangular reinforced concrete squat walls,"Ph.D. thesis, Nanyang technological university, 2017.

[13] Park, R. and T. Paulay, Reinforced Concrete Structures. 1975: Wiley.

[14] Kent, D.C. and R. Park, Flexural members with confined concrete. Journal of the Structural Division, 1971. 97(7): p. 1969-1990.

[15] Barth, K.E. and H. Wu, Efficient nonlinear finite element modeling of slab on steel stringer bridges. Finite elements in analysis and design, 2006. 42(14-15): p. 1304-1313.

[16] Chen, W.F., Plasticity in Reinforced Concrete. 2007: J. Ross Pub.

[17] Hibbitt, K. and Sorensen, ABAQUS/Standard User's Manual. 2001: Hibbitt, Karlsson & Sorensen.

[18] Wahalathantri, B., et al. A material model for flexural crack simulation in reinforced concrete elements using ABAQUS. in Proceedings of the first international conference on engineering, designing and developing the built environment for sustainable wellbeing. 2011. Queensland University of Technology.

[19] Khatami, S. and A. Kheyroddin, Investigation of Element Size Effect on the Nonlinear Behavior of Flanged Shear Walls. Modares Civil Engineering journal, 2012. 12(1): p. 27-37.

[20] Khaloo, A. R., Tabiee, M, Abdoos, H. Analytical study of distribution of shear lag-induced stress in non-rectangular reinforced concrete shear walls, 12th international congress on civil engineering, Mashhad, Iran. 2021: p. 8 [In Persian].